0273-2289/97/63–65—0541$12.00

Fumaric Acid Production in Airlift Loop Reactor with Porous Sparger

JIANXIN DU,*[,1] NINGJUN CAO,[1] CHENG S. GONG,[1] GEORGE T. TSAO,[1] AND NAIJU YUAN[2]

[1]*Laboratory of Renewable Resources Engineering, 1295 Potter Center, Purdue University, West Lafayette, IN 47907; and* [2]*Department of Chemical Engineering, Tsinghua University, Beijing, P. R. China, 100084*

ABSTRACT

Airlift loop reactors with porous spargers were investigated and used in the process of fumaric acid production by *Rhizopus oryzae ATCC 20344*. In order to enhance oxygen mass transfer, which is very important for organic acid production, two kinds of porous spargers (stainless steel membrane tube and porcelain tube) were examined. Gas holdup, liquid circulation velocity, mixing time, bubble size, and bubble rise velocities were measured in a 50 L rectangular airlift loop reactor with different ratios of the cross-sectional area of the riser and downcomer. The local volumetric mass transfer coefficient (K_La) was also measured in the gas sparger zone. The results indicated that high K_La and excellent hydrodynamics can be obtained in the airlift loop reactor with a porous sparger. A 10 L laboratory airlift loop reactor was employed for the fumaric acid fermentation. Results showed that the turbulence of two-phase flow in the airlift loop reactor not only produced favorable conditions for mass transfer, but was also useful for forming and suspending small, well-distributed mycelial pellets (1~2 mm). A production rate of up to 0.814 g/L/h and efficiency yield of 50.1% (w/w) was obtained in the airlift loop reactor. The performance was compared with the typical stirred tank fermentor fermentation results.

Index Entries: Airlift loop reactor; fumaric acid; bubble characteristic; mass transfer coefficient; porous sparger, mycelial pellet; *Rhizopus*.

*Author to whom all correspondence and reprint requests should be addressed.

INTRODUCTION

Fumaric acid is a naturally occurring four-carbon dicarboxylic acid that has many potential applications, such as in the manufacture of unsaturated polyester resins in furniture lacquers, as a food acidulent, and in quick-setting inks *(1)*. Fumaric acid can be produced either chemically or biologically. Many strains of mycelial fungi, especially those belonging to the genus *Rhizopus*, are known to produce appreciable quantities of fumaric acid by utilizing either glucose or xylose *(2,3)*. Because of the ability of *Rhizopus* to fix carbon dioxide and combine it with the metabolic intermediate, pyruvic acid, the high weight yield of up to 93% of fumaric acid from glucose can be achieved.

Fumaric acid is known to be a strong inhibitor of its own production. Therefore, in a typical fumaric acid fermentation, calcium carbonate is usually added to neutralize the acid produced and maintain the fermentation broth at a controlled pH. Calcium fumarate, instead of fumaric acid, is obtained. When fumaric acid production is developed in the conventional stirred tank reactor, the formation of calcium fumarate can cause a drastic change of hydrodynamic conditions of the fermentor. This can result in the premature termination of operation caused by the failure of agitators. On the other hand, the cells of *Rhizopus* tend to grow into large mycelial pellets or clumps, which result in the limitation of oxygen and substrate mass transfer, and encouraged ethanol instead of fumaric acid formation. Fumaric acid production is essentially an aerobic process; it is recognized that the metabolic pathway may shift more toward ethanol formation under oxygen-starved conditions and result in low fumaric acid yield. Jiang *(4)* found that with the increasing air flow rate, the fumaric acid production rate increased, and corresponding ethanol production decreased considerably in a 1 L stirred tank reactor. It is important that the choice and/or design of a suitable bioreactor for fumaric acid production should place emphasis on better hydrodynamics and high oxygen mass transfer rate in order to obtain a high yield and productivity.

The airlift loop reactor has been widely investigated in recent years. It offers several advantages over the traditional bubble column and stirred tank reactor, including the ease of construction and operation, lower energy consumption, lower shear rates, as well as its good hydrodynamics and mass transfer characteristics. Therefore, this type of reactor has been widely employed in industrial applications that require high mass transfer and good dispersion; it is more notable in large scale fermentation industries *(5–7)*. Previously, it has been shown that it is possible to suspend solid particles with a density as high as 2800 kg/m^3 at a solid content of 300 g/L in an airlift loop reactor *(8)*. This indicates that airlift loop reactors are suitable for cultures containing solid particles and mycelial pellets.

Some researchers have studied the cultivation of mycelial fungi in airlift loop reactors. Trager et al. *(9)* used a simple laboratory airlift fermentor to produce gluconic acid with *Aspergillus niger*, and found that smaller pellets were obtained as a result of low stress conditions, as compared to the stirred tank. Okabe et al. *(10)* used an airlift bioreactor in which the top and bottom of the draft tube were covered with stainless steel sieves (four meshes) for the production of itaconic acid by *Aspergillus terreus*. The results showed that the itaconic acid production rate was 100% greater than that of a jar fermentor.

In this study, the authors examined two laboratory-constructed airlift reactors equipped with internal loop and porous gas spargers with 10 and 50 L of working volume, respectively. In the 50 L reactor, bubble characteristics of different regions were measured by means of a dual-probe automatic measurement system that was controlled by an on-line computer. The experimental measurements comprised bubble size, bubble rising velocity, and gas holdup in the riser and downcomer. In order to obtain a better understanding of the hydrodynamics, the liquid circulation velocity, the mean circulation time, and the mixing time were systematically measured in a broad operation range, using the conductive tracking approach. The mass transfer coefficients (K_La) in the gas sparger zones were also studied using a dissolved-oxygen probe to demonstrate the advantages of porous spargers. In addition, fumaric acid production was carried out in the 10 L airlift loop reactor with controlled temperature; results obtained were compared to those with stirred tank reactor.

MATERIALS AND METHODS

Description of Airlift Loop Reactors

50 L Airlift Loop Reactor

The configuration of an airlift loop reactor with a 50 L working volume for the hydrodynamic measurements is shown in Fig. 1. This reactor was constructed with polymethyl methacrylate that has a rectangular cross-section for the installation of conductivity probes at different axial positions. A baffle divides the rectangular part into two sections: the riser and the downcomer. The position of the baffle is designed to be mobile so the ratios of different cross-sectional areas of the riser and downcomer can be obtained in one reactor. The top part (head), where gas–liquid separation occurs, is designed for good circulation and mixing of gas and liquid. The head portion of the reactor, the so-called gas-liquid separator, can be operated in either the closed or opened modes, as shown in Fig. 1. At the bottom of the reactor, a stainless steel membrane tube (pore size, 30~40 μm; diameter, 40 mm; and length, 120 mm) was used as the gas sparger, which can distribute air evenly into the reac-

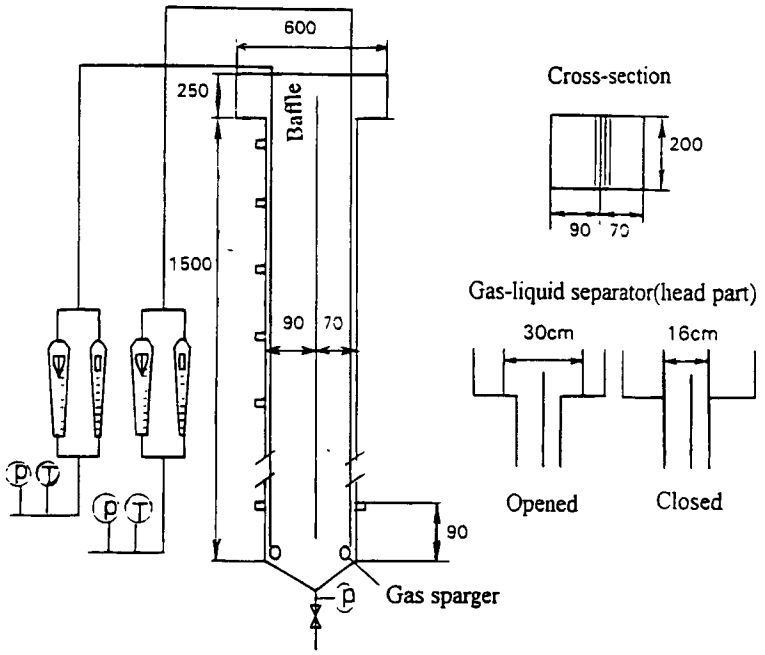

Fig. 1. The configuration of 50 L airlift loop reactor. *See* Table 1 for dimensions.

tor as tiny air bubbles of 1~2 mm in diameter. Dimensions of the reactor are given in Table 1.

10 L Airlift Loop Reactor

The configuration of the 10 L working volume airlift loop reactor with attachments for the fumaric acid production is shown in Fig. 2. This 10 L reactor was constructed of Pyrex glass pipe and equipped with stainless steel fittings. A concentric draught tube inside the reactor was used as the riser section to form an inner gas-liquid loop. This reactor contains several ports for installing the dissolved oxygen, pH probes, and temperature sensor for addition of nutrient medium, antifoam, neutralization agent, and for removing exhaust gas. By circulating water through a heat exchanger inside the reactor, the temperature during fermentation can be controlled. A porcelain tube (pore size, 80 μm; diameter, 40 mm; and length, 50 mm. Fisher Scientific Co.) was inserted into the bottom of the reactor as the air sparger. The dimensions of this 10 L reactor are also given in Table 1.

Dual-Probe Conductivity Sensor

The schematic diagram of a dual-probe conductivity sensor made in the laboratory is shown in Fig. 3. The use of the conductivity probe has many advantages for measuring the bubble characteristics in two-phase flow, including fast response, high sensitivity, ease of operation, and ease

Table 1
Geometrical Characteristics of Airlift Loop Reactors (ALRs)

Geometrical Parameter	ALR for Hydrodynamics Measurement	ALR for Fumaric Acid Production
Working Volume	50 L	10 L
Cross-Sectional Shape	Rectangular	Cylindrical
Total Reactor Length	1750 mm	1165 mm
Cross-Sectional Size	Length: 200 mm	Diameter: 100 mm
	Width: 160 mm	
Length of Baffle	1500 mm	-
Length of Draft Tube	-	900 mm
Diameter of Draft Tube	-	Diameter: 80 mm
S_r/S_d[a]	1.07	1.78
	1.58	
	2.44	
	4.17	
Gas-Liquid Separator	Closed[b]: 200×160×250 mm^3	Diameter: 153 mm
	Opened[c]: 200×300×250 mm^3	Height: 250 mm
Air Sparger	Stainless Steel Membrane Tube	Porcelain Membrane Tube

[a]Ratio of cross-sectional area of riser and downcomer.

[b]Means gas-liquid separator has the same cross-sectional area as the main part of the reactor.

[c]Means gas-liquid separator has larger cross-sectional area than that of the main part of the reactor.

of control by a computer *(11)*. Because of its high hardness, tungsten filament (diameter = 8×10^{-5} mm) was selected as the electrode. Glass capillary (diameter = 0.3 mm) was employed as an insulating sleeve, that made the drying of the probe easier. The measurement results indicate that this dual-probe sensor can measure tiny bubbles as small as 0.6 mm in diameter with satisfactory stability and reproducibility *(11)*. Using this type of dual-probe automatic measurement system controlled by an on-line computer in an airlift loop reactor has not been reported in the literature.

Micro-organism and Inoculum

Rhizopus oryzae ATCC 20344, purchased from American Type Culture Collection (Rockville, MD), was chosen for this study because of its ability to produce fumaric acid from glucose *(12)*. The culture was propagated on YMA (Difco) agar plates. After the spores formed, the agar plates were

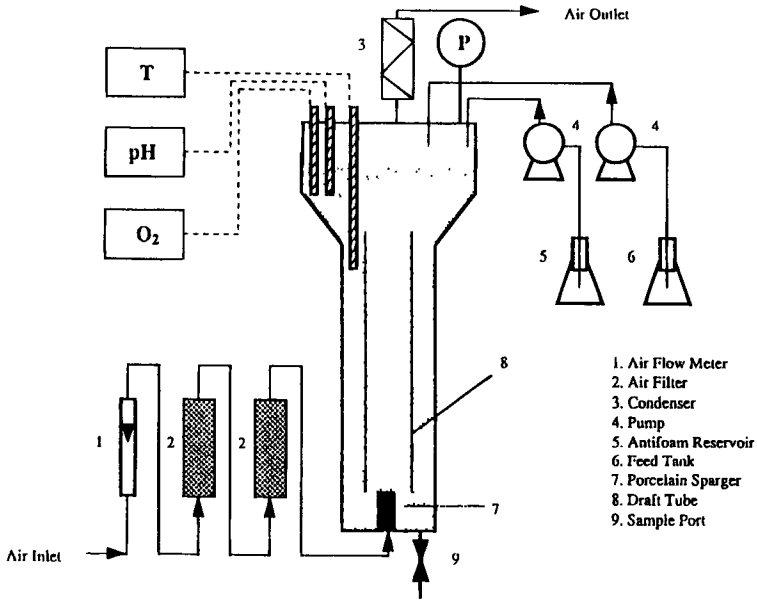

Fig. 2. Schematic diagram of airlift loop reactor (10 L) for fumaric acid production.

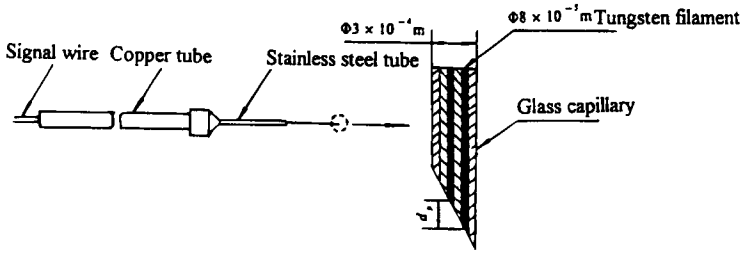

Fig. 3. Schematic diagram of dual-probe conductivity sensor.

maintained at 4°C. For inoculation, the agar plates containing sporangiospores were washed with sterile water to obtain the spore suspension. The spores were then collected by filtration and used as inocula.

Cultivation

Because *Rhizopus oryzae* grows slowly using xylose as the carbon source, small pellets can be formed in the medium containing xylose *(13)*. In order to obtain small- and uniform-sized pellets in the airlift loop reactor, preculture was performed in the flasks on the shaker. Cultivation medium consisted of 50 g xylose, 2 g urea, 0.6 g KH_2PO_4, 0.25 g $MgSO_4 \cdot 7H_2O$, and 0.088 g $ZnSO_4 \cdot 7H_2O$, per liter of distilled water. The spore solution was inoculated into 2500-mL Erlenmeyer flasks containing 1000 mL sterilized cultivation medium. Incubation was carried out at

30°C and 150 rpm in a gyratory shaker for about 2 d. The mixture of filamentous fungi and small fluffy pellets with hairy surfaces were obtained for fermentation studies.

Fermentation

Mycelial pellets from flask cultures were harvested and transferred into the 10 L airlift loop reactor containing fermentation medium that consisted of 100 g glucose, 0.5 g urea, 0.6 g KH_2PO_4, 0.25 g $MgSO_4 \cdot 7H_2O$, and 0.088 g $ZnSO_4 \cdot 7H_2O$, in one L distilled water. The fermentation was operated at 35°C with an air flow rate of 8.5 L/min (about 1 vvm). $CaCO_3$ was added whenever needed, to maintain pH in the broth at around 5.

Analytical methods

High Performance Liquid Chromatography (HPLC)

High Performance Liquid Chromatography (HPLC) with an RI detector, an automatic injector, and an integrator (Hitachi, Tokyo, Japan) was used to determine sugar, fumaric acid, and by-product concentrations. The mobile phase was 0.005*M* H_2SO_4 at a flow rate of 0.8 mL/min through a BioRad HPX-87H Ion-Exclusion column (BioRad Laboratory, Hercules, CA) at 60°C.

Final Fumaric Acid Concentration

Because of the low solubility of calcium fumarate (~25 g/L at 35°C), fumarate may precipitate during fermentation. In order to obtain an accurate total amount of the fumaric acid produced, water was added to the broth after fermentation until the fumarate concentration was lower than its solubility. This was followed by heating the broth for 1 h at 80°C. Samples were collected for analysis.

RESULTS AND DISCUSSION

Bubble Characteristics in Airlift Loop Reactor

Previous studies on the hydrodynamics of the airlift loop reactor have been based mostly on the concept of viewing the reactor as a whole. Very little attention was focused on the local properties that resulted in many problems that hindered further applications of the airlift reactor in the industry. For this reason, local gas holdup, bubble size, and bubble velocity were measured by a dual-probe conductivity sensor in both the riser and the downcomer in the 50 L airlift loop reactor.

In an air-water system, when a single nozzle sparger or perforated ring sparger was employed, large spherical-capped bubbles (5~10 mm in diameter) were predominant in the riser section, and many larger bubbles were trapped in the downcomer as well. As the superficial air velocity increased, bubbles in both the riser and the downcomer coalesced rapidly

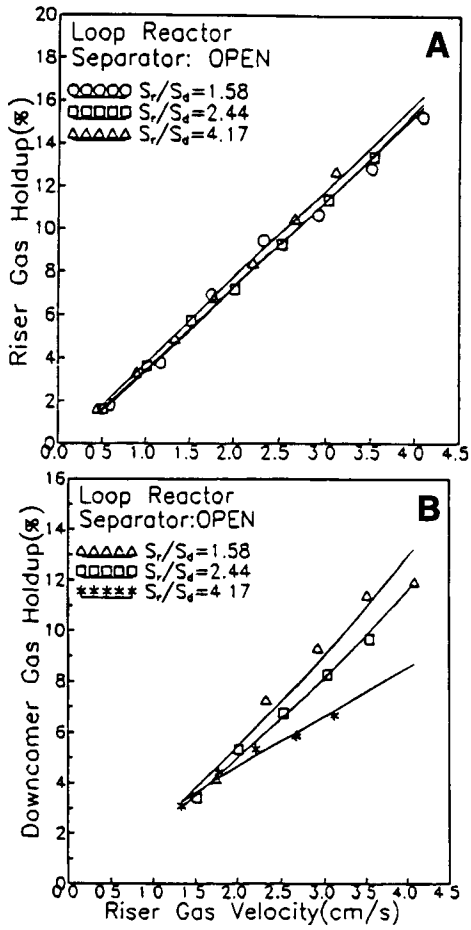

Fig. 4. Effects of superficial air velocity on the mean gas holdup in 50 L airlift loop reactor. **(A)** The riser. **(B)** The downcomer.

to form large bubbles. Some of the bubbles can be as large as the width of the reactor. In this study, very small and uniform bubbles were formed from the porous holes of the stainless steel membrane sparger. Bubble diameters 1–5 mm were observed along the length of the riser.

Gas holdup is one of the most important parameters characterizing the performance of the airlift loop reactor. Effects of superficial air velocity on the mean gas holdup in the riser and the downcomer is shown in Fig. 4a and 4b. It can be seen that gas holdup in the riser displayed the same principle at different riser-downcomer cross-sectional area ratios (S_r/S_d); a linear increase in gas holdup was found with an increasing superficial gas velocity. In the downcomer, gas holdup was a function of S_r/S_d and tended to decline with increasing S_r/S_d. Liquid circulation velocity increased with increasing S_r/S_d because of the rising of circulation drive force. Higher gas holdup was obtained in this study when compared to the data obtained by Kawase and Moo-Young *(14)*.

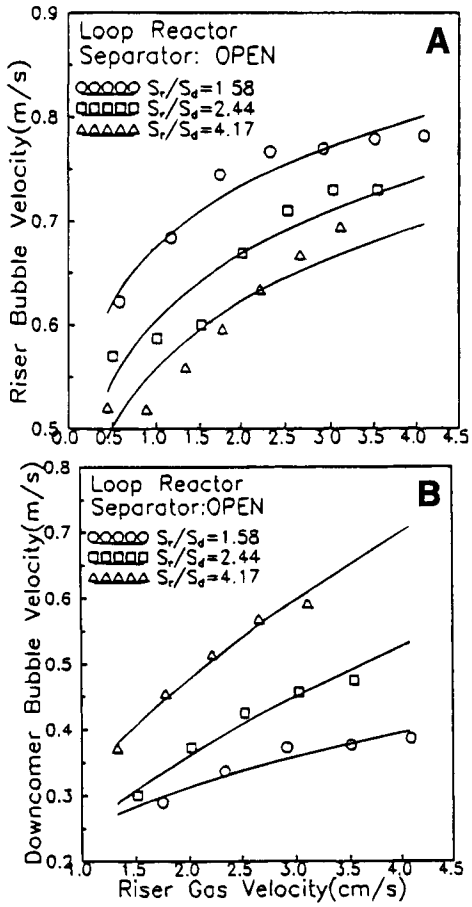

Fig. 5. Effects of superficial air velocity on the mean bubble velocity in 50 L airlift loop reactor. **(A)** The riser. **(B)** The downcomer.

Gas-liquid relative velocity and bubble size are two main parameters influencing gas-liquid mass transfer. Figures 5a and 5b show the effects of the superficial gas velocity in the riser on bubble velocity. The effects of S_r/S_d and riser superficial gas velocities on bubble size in the riser and downcomer are given in Figures 6a and 6b. In the riser, bubble size increased with an increase in both S_r/S_d and riser superficial gas velocity. In the downcomer, bubble size remained almost constant with increasing riser superficial gas velocity at lower values of S_r/S_d, and decreased at higher values of S_r/S_d because bubble breakup frequency increased with higher liquid circulation velocity.

Liquid Circulation Velocity and Mixing

Liquid circulation velocity is another important parameter affecting the behavior of the airlift loop reactor. Based on previous observation, liquid circulation velocity not only depends on the gas flow rate, but also is

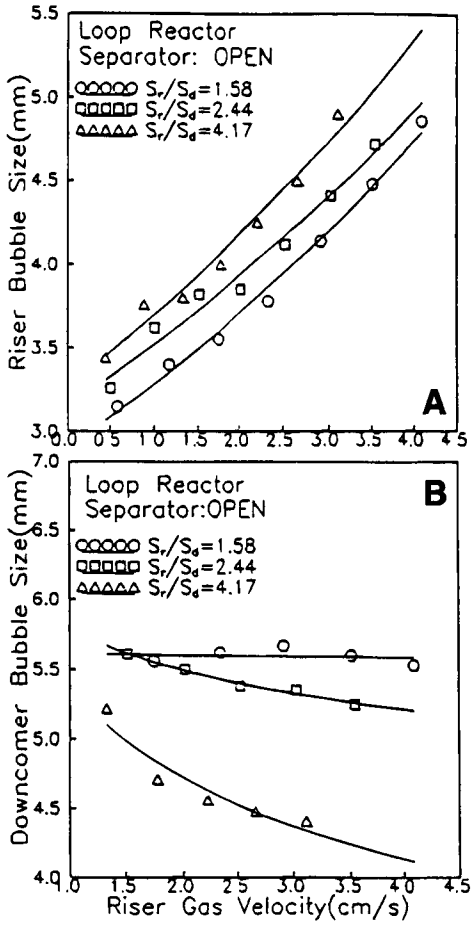

Fig. 6. Effects of superficial air velocity on the mean bubble diameter in 50 L airlift loop reactor. **(A)** The riser. **(B)** The downcomer.

sensitive to the structure of the gas-liquid separator (head part) *(11)*. "Opened mode," which means the cross section of the head is larger than that of the main part of the reactor, accounts for the expected high liquid circulation velocity. This is a result of a sufficient gas-liquid separation region in the head. Figure 7 shows the effect of riser superficial air velocity on the liquid circulation velocity in the riser with the head opened. Higher liquid velocity was obtained at a lower S_r/S_d because of a larger difference of gas holdup in the riser and downcomer. There was no significant difference in liquid circulation time at riser superficial gas velocity above 3.0 cm/s (Fig. 8). However, liquid mixing time decreased with increasing riser superficial air velocity and S_r/S_d, because of the enhancement of gas-liquid turbulence (Fig. 9).

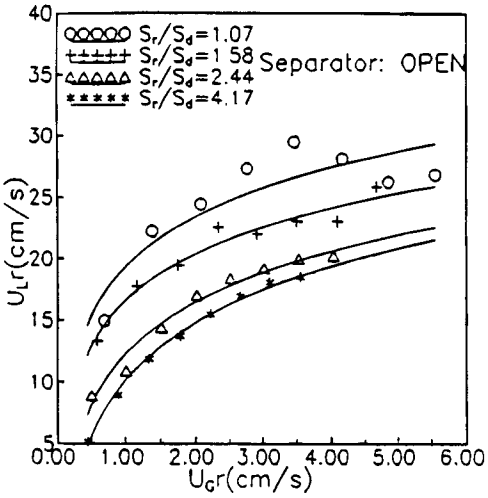

Fig. 7. Effects of riser superficial air velocity on the liquid circulation velocity in the riser of 50 L airlift loop reactor.

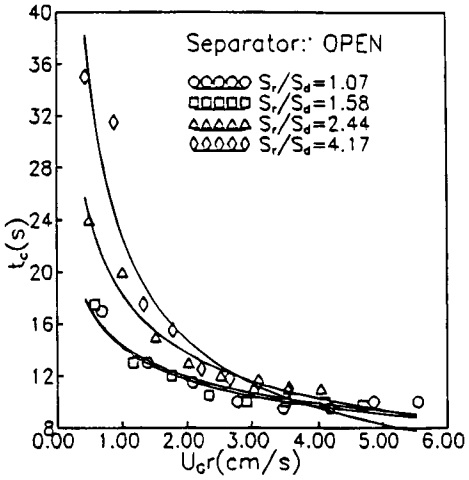

Fig. 8. Effects of riser superficial air velocity on the liquid circulation time of 50 L airlift loop reactor.

Mass Transfer Characteristics in Airlift Loop Reactor

The volumetric mass transfer coefficient (K_La) in the airlift loop reactor is affected by many factors, such as; liquid phase diffusibility, bubble and liquid velocity, bubble size and its distribution, gas holdup, and gas-liquid turbulence. However, K_La is very sensitive to bubble size that affects mass transfer coefficient (K_L) and gas-liquid interfacial area per unit volume (a). When a stainless steel membrane sparger is used in the airlift loop reactor, small bubbles were obtained, especially in the gas sparger zone. For the air-water system, the initial bubble size formed from the membrane sparger

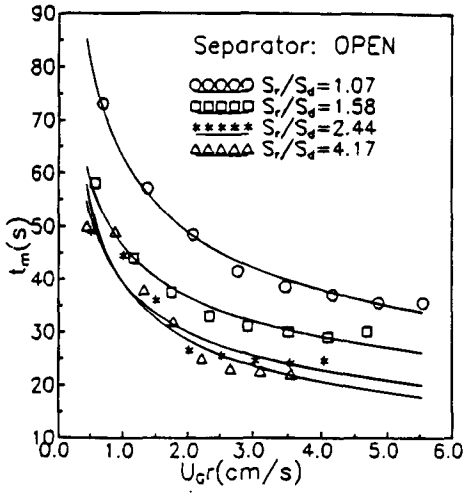

Fig. 9. Effects of riser superficial air velocity on the mixing time of 50 L airlift loop reactor.

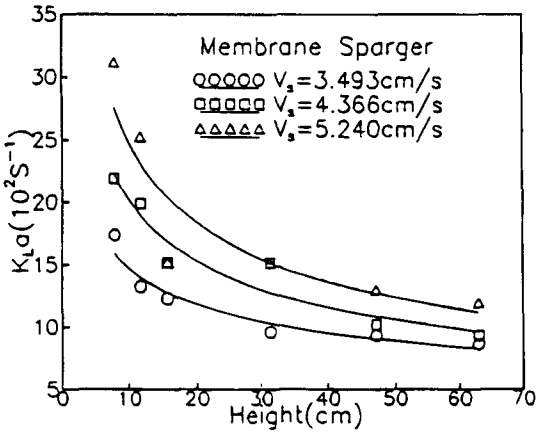

Fig. 10. Effects of height on volumetric mass transfer coefficient in sparger zone of 50 L airlift loop reactor.

was in the range of 1~2 mm. In the gas sparger zone (height of 40 cm in the 50 L airlift loop reactor), the bubble size increased rapidly along the axial positions leading to a decrease of K_La. K_La measured by a dissolved oxygen probe in the gas sparger zone as a function of height, is given in Fig. 10. It can be seen that at superficial air velocity of 5.24 cm/s, K_La decreased from 0.3 to 0.14 S^{-1}. For comparison, the experimental data obtained for air-water system from this work, results reported by Kawase and Moo-Young *(15)* and by Shah et al. *(16)*, using single nozzle sparger, were plotted and compared and are shown in Fig. 11. It was obvious that because of the use of a membrane sparger, K_La increased 3~4 times, compared with K_La found using a single nozzle sparger.

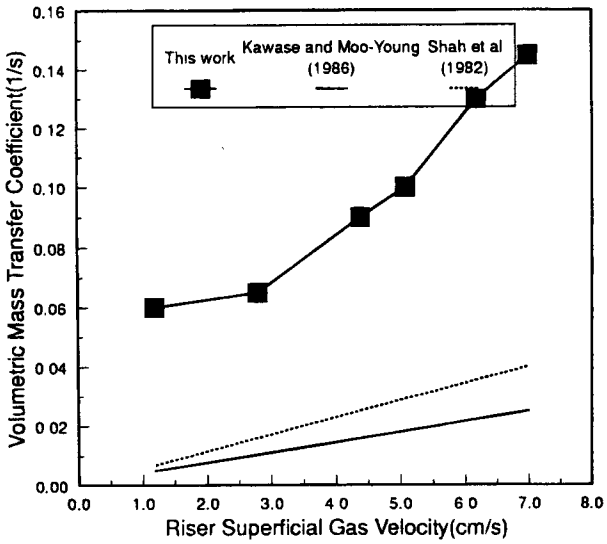

Fig. 11. Comparison between volumetric mass transfer coefficients obtained from published data with single gas sparger and with stainless steel membrane gas sparger in 50 L airlift loop reactor.

Mycelial Pellet Formation in Airlift Loop Reactor

When filamentous fungi were grown in submerged cultures, the type of growth varied from the pelletes to filamentous forms and/or a mixture of both forms. Mycelial pellets consist of compact discrete masses of hyphae, and the filamentous forms consist of homogeneous hyphae suspension were distributed throughout the medium. The filamentous form is preferred for fumaric acid production because of its good properties of oxygen and substrate mass transfer. However, when $CaCO_3$ was added to neutralize the acid produced, the filamentous fungi coagulated to form large clumps of mass that were easily precipitated to the bottom of the reactor. Therefore, the small pelleted form is preferred for fermentation. After cultivation, the mixture of filamentous and small fluffy pellets was transferred to an airlift loop reactor containing fermentation medium containing a limited quantity of nitrogen source (0.5% urea) in order to shift the organism from growth stage to acid production stage. When the air rate was 1 vvm, very small and uniform pellets formed with an average diameter of about 2 mm. Based on the visual observation, the small pellets in the airlift loop reactor were easily suspended and circulated and very well distributed in the entire zone of the reactor. During mechanically agitated fermentation in a stirred tank reactor, some very large mycelial clumps were formed whereas others retained their original mycelial form as a result of shear stress exerted by the agitator. The formation of large mycelial pellets often led to premature termination of fermentation (2). Another advantage of operating in small pelleted form was a low viscosity

of broth that not only benefited mass transfer, but also avoided foaming as compared to filamentous form.

Fumaric Acid Production in an Airlift Loop Reactor

Two pathways, oxidative and reductive, are involved in fumaric acid metabolism in fungi. The oxidative pathway (TCA cycle) will generate one mole of fumarate per mole of glucose consumed. During active cell growth, however, this pathway cannot lead to the accumulation of fumarate. The generated fumarate was utilized for biosynthesis of cell constituents *(2)*. On the other hand, the accumulation of fumaric acid is dependent on the operation of the reductive branch of the TCA cycle *(17,18)*. The carbon dioxide-fixing reductive branch is capable of producing two moles of fumarate per mole of glucose consumed. The enzyme responsible for fumarate accumulation in *Rhizopus* is pyruvate carboxylase (EC 6.4.1.1) *(19)*. This enzyme catalyzed the ATP-dependent condensation of pyruvate and CO_2 to form oxaloacetic acid, the key intermediate of TCA cycle. The ability of fungi, such as *Rhizopus*, to incorporate CO_2 into the reductive branch of oxidative pathway render them the ability to produce organic acids in very high yield with fumaric acid as the major acid product *(20)*.

By limiting the nitrogen source, *Rhizopus* cell growth can be kept minimal. During this non-growth stage, fumaric acid can be accumulated with a maximum yield of 2 moles per mole glucose consumed or 1.29 g fumarate per g of glucose consumed on the basis of weight *(17)*. In reality, the reductive bypass requires the supply of NADH from TCA cycle. Therefore, the obtainable yield is about 1.45 moles of fumarate from each mole of glucose (as much as 0.93 g per g of glucose consumed) *(2)*.

Figure 12 shows the time course of fumaric acid fermentation in 10 L airlift loop reactor. It can be seen that the final fumaric acid concentration reached 37.8 g/L after 46 h, and the productivity and efficiency yield were 0.814 g/L/h and 50.1%, respectively. The concentration of ethanol produced in the broth was under 10 g/L. The comparison of the results in the airlift loop reactor and stirred tank was summarized in Table 2. Noticeably, the productivity of fumaric acid in the airlift loop reactor was higher than in the stirred tank reactor. Furthermore, the maximum ethanol concentration in the stirred tank reactor reached 20g/L, which was twice as as that in the airlift loop reactor. The measured results of dissolved oxygen show that nearly 90% of saturation was obtained in the airlift loop reactor throughout the entire course of fermentation at an air supply of 1 vvm.

CONCLUSION

A dual-probe automatic measurement system controlled by an online computer was used to measure the bubble characteristics in the airlift loop reactor. The results indicated that K_La in the gas sparger zone

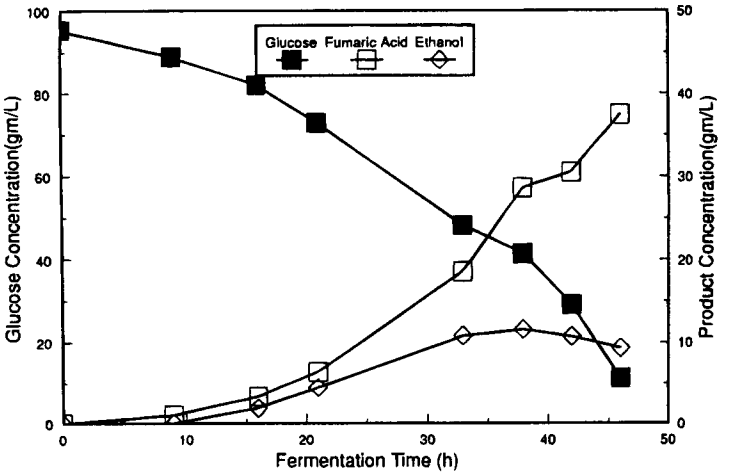

Fig. 12. Time course of fumaric acid fermentation in 10 L airlift loop reactor with porous gas sparger. Air flow rate: 1 vvm; Temperature: 35°C.

Table 2
Comparison of Fumaric Acid Production by *R. Oryzae* in Different Fermentors

Process	Airlift Loop Reactor	Stirred Tank Fermentor
Volume(L)	10	6.5
Neutralizing Agent	$CaCO_3$	$CaCO_3$
Initial Glucose(g/L)	95	100
pH	4.0~5.0	5.0
Fermentation Time(h)	46	89
Air Flow Rate(L/L/min)	0.9	2.0
Stirring Speed(rpm)	-	600
Yield(%[a])	75.4	60
Productivity(g/L/h)	0.814	0.66

[a]Yield = (maximum g/L of fumaric acid)/(g/L of glucose consumed)

decreased rapidly along the axial position because of the increase in bubble size. By employing the porous gas sparger, K_La in the airlift loop reactor increased significantly compared with K_La found using single nozzle spargers. The results of fumaric acid fermentation show that the hydrodynamics in the laboratory airlift loop reactor with porous sparger produced favorable conditions for mass transfer. In addition, it is useful for forming small uniform mycelial pellets. Higher production rates and product yields were obtained in the airlift loop reactor than in the typical stirred tank fermentor. Airlift loop reactors have the potential for application in a larger scale fungus fermentation system.

ACKNOWLEDGMENTS

This research was supported in part by Division of Biological and Critical System, National Science Foundation grant BES-9412582.

NOMENCLATURE

a	gas-liquid interfacial area per unit volume, m^2/m^3
K_L	mass transfer coefficient, m/s
K_La	volumetric mass transfer coefficient, 1/s
S_r/S_d	ratio of cross-sectional area of riser and downcomer
t_c	liquid circulation time, s
t_m	liquid mixing time, s
U_Lr	liquid circulation velocity, cm/s
U_Gr	riser gas velocity, cm/s
V_s	superficial gas velocity, cm/s.

REFERENCES

1. Robinson, W. D. and Mount, R. A. (1981), in *Kirk-Othmer Encyclopedia of Chemical Technology, Vol. 14*, Grayson, M. and Eckroth, D., eds., Wiley, New York, p. 770.
2. Rhodes, R. A., Lagoda, A. A., Misenheimer, T. J., Smith, M. L., Anderson, R. F., and Jackson, R. W. (1962), *Appl. Microbiol.* **10,** 9–15.
3. Kautola, H. and Linko, Y. (1989), *Appl. Microbiol. Biotechnol.* **31,** 448–454.
4. Jiang,Y. H. (1995), M. S. thesis, Purdue University.
5. Bayer, T., Zhou, W., Holzhaner, K., and Schugerl, K. (1989), *Appl. Microbiol. Biotechnol.* **30,** 26–33.
6. Siegel, M. H., Hallaile, M., and Merchuk, J. C. (1988), Upstream Process Equipment and Techniques, Alan R. Lisss Inc., New York, pp. 79–124.
7. Konig, B., Schugerl, K., and Seewald, C. (1982), *Biotechnol. Bioeng.* **24,** 259–280.
8. Heck, J. and Onken, U. (1982), *Chem. Eng. Sci.* **42,** 1211–1212.
9. Trager, M., Qazi, G. N., Onfen, U. and Chopra, C. L. (1989), *J. Fermen. Bioeng.* **68,** 112–116.
10. Okabe, M., Ohta, N., and Park, Y. (1993), *J. Fermen. Bioeng.* **76,** 117–122.
11. Du, J. X. (1995), Ph. D. thesis, Tsinghua University, P. R. China.
12. Yang, C. W. (1994), Ph. D. thesis, Purdue University.
13. Yang, C. W., Lu, Z. J., and Tsao, G. T. (1995), *Appl. Biochem. Biotechnol.* **51/52,** 57–71.
14. Kawase, Y. and Moo-Young, M. (1986), *Chem. Eng. Commun.* **40,** 67–83.
15. Kawase, Y. and Moo-Young, M. (1988), *Chem. Eng. Res. Des.* **66,** 284–288.
16. Shah, Y. T., Kelkar, B. G., Godbole, S. P., and Deckwer, W. D. (1982), *AIChE J.* **28,** 353–379.
17. Gangl, I. C., Weigand, W. A., and Keller, F. A. (1990), *Appl. Biochem. Biotechnol.* **24/25,** 663–677.
18. Peleg, Y., Battat, E., Scrutton, M. C., and Goldberg, I. (1989), *Appl. Microbiol. Biotechnol.* **32,** 334–339.
19. Kenealy, W., Zaady, E., Du Preez, J. C., Stieglitz, B. and Goldberg, I. (1986), *Appl. Environ. Microbiol.* **52,** 128–133.
20. Overman, S. A. and Romano, A. H. (1969), *Biochem. Biophys. Research Commun.* **37,** 457–463.